An optimal and Efficient PV System using two 2-level Cascaded 3-level inverter for Centrifugal Pump

Ramulu Chinthamalla, *Member IEEE*, K. Shivaji Ganesh and Sachin Jain
Department of Electrical Engineering,
National Institute of Technology,
Warangal - 506004, Telangana State, INDIA
Email: rnitchinthamalla@nitw.ac.in, ksganesh021@gmail.com, jsachin@nitw.ac.in

Abstract—**In this paper a three-phase single-stage integrated multilevel inverter PhotoVoltaic (PV) fed Induction Motor (IM) pump drive system is presented. The proposed system uses two 2-level cascaded H-bridge inverters for the 3-level output which is fed from two independent PV sources. Usage of cascaded inverter configuration eliminates the problem of neutral point fluctuations, does not require fast recovery neutral clamping diodes & high value capacitor when compared with conventional multilevel inverter configurations like 3-level Neutral-Point Clamped [NPC] inverter and Flying Capacitor (FC) inverter. Further, it requires only two isolated DC power sources in comparison with 3-level H-bridge configuration which demands three sources. The given system uses both the PV sources efficiently which may help in optimal sizing of PV source with respect motor load requirements. Further, for optimal utilization of PV source a Maximum Power Point Tracking [MPPT] algorithm is also employed. This paper also gives a detailed yet simple mathematical model for the cascaded inverter and its integration with PV module for simulation in Matlab-Simulink. Also a simple Sinusoidal Pulse Width Modulation [SPWM] technique is used for switching of the inverter. The proposed system has the advantages of simple *V/f* control integrated with MPPT algorithm. *V/f* control retains maximum torque capability of the motor which further helps in optimum utilization of the PV-source and the IM. The simulation results of the proposed system under various environmental conditions has been discussed and presented in the paper.**

Keywords—centrifugal pump; maximum power point tracking; cascaded MLI Inverter, photovoltaic cell.

I. INTRODUCTION

The fast increasing demand of electrical power, due to the growth of population and its requirements for modern industrial & domestic needs, has motivated a lot of research to find out alternative electrical energy solutions. Today, most of the research is focused on the effective utilization of non-conventional energy sources. Of all the existing non-conventional sources of energy, solar PhotoVoltaic (PV) technology is popularly used as it has many advantages [1-2]. The benefits of solar PhotoVoltaic panel are: it absorbs the everlasting solar energy at free of cost and it is eco-friendly without generating any kind of pollution into the atmosphere and offers low noise and low maintenance, when compared with conventional energy sources. It directly converts the solar energy from Sun into DC electric power. The generated DC power from PV array is conditioned or transformed in required form using Power Conditioning Unit (PCU). The PCU can be any inverter or converter circuit depending on application of PV system. Based on number of levels at the output inverters can be broadly classified into two types: 2-level inverter and Multi-Level Inverter (MLI). In recent years, MLI [3] have attracted the attention of the researchers and manufactures due to their simplicity and user friendly features over conventional 2-level inverter with high quality power output. High magnitude and quality output voltage can be obtained using more number of low value independent DC sources with reduced value of dv/dt stress on the switches. These advantages attracts the application of Multi-Level Inverters (MLIs) configuration for drive & PV applications [4-8]. There are several MLI configurations available or given in the literature from the past two decades. Most of them are based on three basic configurations: Neutral Point Clamped (NPC) (or diode clamped) [9-10], Flying Capacitor (FC) (or capacitor clamped) [11] and Cascaded H-bridge inverter with separate DC-sources [12-13]. Among these configurations, 3-level inverter configuration using cascaded two 2-level inverter [14] is used for investigation. It has the advantages of no requirement for additional clamping diodes, eliminates neutral point fluctuations problem when compared with conventional NPC 3-level MLI. Further, it eliminates the requirement of large value capacitors when compared with Flying Capacitor or NPC. It also requires only two isolated DC- power supplies when compared to cascaded H-bridge 3-level configuration, which needs three isolated DC-power supplies. It not only achieves high power ratings, but also enables the use of small renewable energy sources with low output voltage. Renewable energy sources such as PhotoVoltaic, fuel cell etc. can be interfaced with a MLI system for a high power application. In the present paper, a single- stage PV fed water pumping system is proposed. It uses a 3-Ø squirrel cage IM powered by a 3-level cascaded two 2-level inverter as shown in Fig. 1. To improve the performance of an IM and the efficiency of the PV pumping system, carrier wave based Sinusoidal Pulse Width Modulation (SPWM) technique with *V/f* control is employed.

978-1-4799-6373-7/14/$31.00 ©2014 IEEE

It also takes care of MPPT for the PV system. In the proposed system *V/f* is integrated with MPPT technique, which meets the basic requirements of simplicity & cost effectiveness. The given manuscript divided into-sections: First, operation and modelling of the proposed system are presented in section II. Section III describes the control strategy and MPPT algorithm used for the proposed system. Section IV gives the simulation results and analysis for the proposed system. The last section discusses the conclusions.

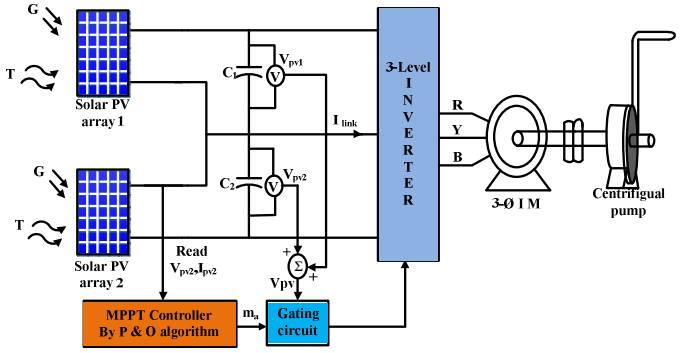

Fig. 1. Block diagram of Single-stage PV powered centrifugal Pump.

II. OPERATION AND MODELLING OF PROPOSED SYSTEM

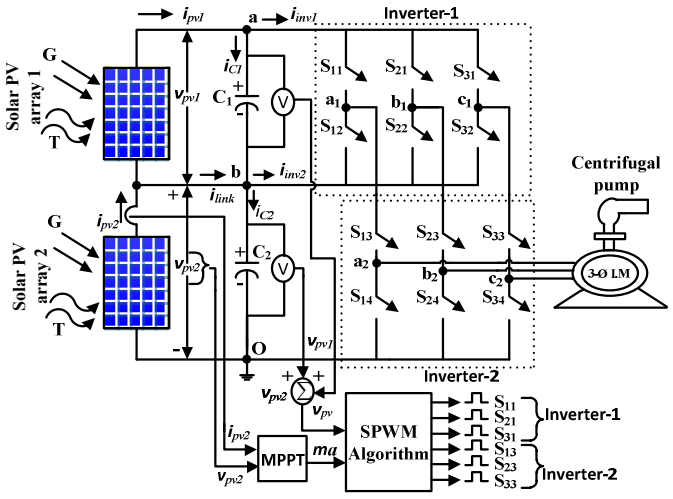

Fig. 2. Schematic diagram of proposed system.

The given system consist of 3-level cascaded inverter [14] integrated with PV sources and three-phase water motor pump as shown in Fig. 2. The generated PV power is conditioned by cascaded 3-level inverter so that it can be utilized by motor effectively. The cascaded MLI inverter configuration [14] also takes care for MPPT required for optimal utilization of the PV source. It is operated using simple Sine Triangle Pulse Width Modulation (SPWM) technique in which both input PV sources are utilized effectively for all values of modulation index (m_a). The switches in the each leg of the inverter are switched by using complementary switching technique. To verify the system operation complete mathematical model for the proposed system was developed. The developed model consist of blocks of two PV sources, 3-level cascaded inverter & motor-pump set as shown in Fig . 1.

A. PV source Model [15]

The solar PhotoVoltaic (PV) system, directly converts the solar energy into electrical energy. The basic element/device in a solar array is the solar cell, which is basically a p-n junction semiconductor device. The electrical equivalent circuit of a solar cell is shown in Fig. 3.

The *i-v* characteristic equation for PV cell is given by

$$i_{pv} = i_L - i_o\left(e^{\frac{q\left(v_{pv}+i_{pv}R_s\right)}{\eta kT}-1}\right) \qquad (1)$$

where i_{pv} is the PV cell current (A), i_L is the photo-current (A), i_o is the diode reverse saturation current (A), η is the diode ideality factor, k is the boltzmann constant (J/K), q is the electron charge (C), T is the panel operating temperature (K), R_s is the PV cell series resistance, v_{pv} is the PV cell voltage (V).

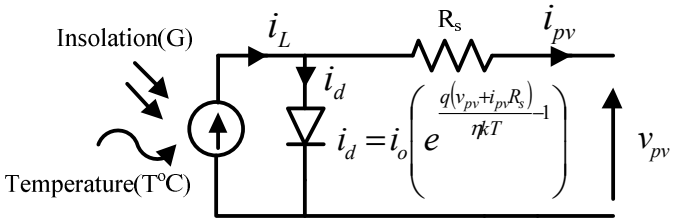

Fig. 3. Equivalent accurate model of PV cell [15]

To model PV source (or PV array), the given *i-v* characteristic equation (1) can be modified with respect to required series-parallel connection of the PV cells. The output of PV arrays 1 and 2 is connected to inverter-1 and inverter-2 with PV-link capacitors C_1 & C_2 respectively. By applying KCL at nodes 'a' & 'b' of inverter (Fig. 2) we have,

$$i_{pv1} = C_1\frac{dv_{pv1}}{dt} + i_{inv1} \qquad (2)$$

$$i_{pv2} = C_2\frac{dv_{pv2}}{dt} + i_{inv2} - i_{C1} + i_{pv1} \qquad (3)$$

where v_{pv1} is the PV array 1 voltage (V), v_{pv2} is the PV array 2 voltage (V), i_{pv1} is the current of PV array 1 (A), i_{pv2} is the current of PV array 2 (A), i_{inv1} is the inverter-1 current (A), i_{inv2} is the inverter- 2 current (A). Integral solutions for the eqn (2) and (3) can be used for the calculation of DC bus capacitor voltage.

B. Three-level cascaded-inverter model

The calculated PV source output voltage are used for the simulation of cascaded inverter. Mathematical model for the inverter is developed by calculating the pole-voltage at the phase output of each-leg in inverter. Pole-voltage in each leg of inverter can be calculated with reference to nodal point 'O', as shown in Fig. 2. The calculated pole-voltage is then used for calculation of phase-voltage as described below. Pole-voltage of inverter-1 with reference to node 'O' in the leg

connected to phase 'a' is denoted by v_{a1o}. Similarly, pole-voltage for leg connected to other phase 'b' and 'c' are denoted as v_{b1o}, v_{c1o}. The pole voltage v_{a1o} can contain two values (v_{pv1}+v_{pv2}) or (v_{pv2}) depending whether s_{11} or s_{12} is turned ON respectively [16]. Thus, it can be denoted mathematical by equation.

$$v_{a1o} = (v_{pv1} + v_{pv2})s_{11} + (v_{pv2})s_{12} \quad (4)$$

where s_{11} and s_{12} have values '1' for turn-on state of respective switch or '0' for turn-off state of respective switch.

Similarly, pole voltage for other phases 'b' & 'c' are given as,

$$v_{b1o} = (v_{pv1} + v_{pv2})s_{21} + (v_{pv2})s_{22} \quad (5)$$

$$v_{c1o} = (v_{pv1} + v_{pv2})s_{31} + (v_{pv2})s_{32} \quad (6)$$

Using the same strategy the pole-voltage for inverter-2 can be determined. Then the pole-voltage for inverter-2 can be written as,

$$v_{a2o} = (v_{pv1} + v_{pv2})s_{11}s_{13} + (v_{pv2})s_{12}s_{13} \quad (7)$$

It can be easily observed from eqn (7) that pole-voltage of inverter-2 attain three values '(v_{pv1}+v_{pv2})', 'v_{pv2}' & '0'. It attains zero voltage when switch s_{13} is turned-off (or have '0') and otherwise, will have same value as v_{a1o}. Expression for pole- voltage at inverter- 2 is also given by

$$v_{a2o} = v_{a1o}s_{13} \quad (8)$$

Same hold true for pole-voltage at other phases. As, motor stator winding is connected to inverter-2, so the pole-voltage of inverter-2 are used for calculation of phase-voltage applied to stator winding. Phase-voltage across the stator winding of induction motor can be calculated by subtracting common-mode voltage from pole-voltage as given below,

$$v_{an} = v_{a2o} - v_{no} \quad (9)$$

v_{no} can be calculated as,

$$v_{no} = \frac{1}{3}(v_{a2o} + v_{b2o} + v_{c2o}) \quad (10)$$

where v_{an} is the motor a-phase voltage; v_{no} is the common-mode voltage. The calculated phase-voltage can again be used for calculation of individual phase currents. Again calculated phase currents can further be utilized for calculation of respective inverter current as described below,

$$i_{inv1} = s_{11}s_{13}i_a + s_{21}s_{23}i_b + s_{31}s_{33}i_c \quad (11)$$

$$i_{inv2} = s_{12}s_{13}i_a + s_{22}s_{23}i_b + s_{32}s_{33}i_c \quad (12)$$

Further, as average value of current through capacitor C_1 & C_2 is zero in a switching cycle, eqn (2) and (3) can further be simplified to,

$$\therefore \; I_{pv1} = I_{inv1} \quad (13)$$

$$I_{pv2} = I_{inv2} + I_{inv1} \quad (14)$$

where 'I' represents average value over a switching cycle.

C. Modelling of 3-Φ IM with Centrifugal water pump load

Dynamic d-q model for 3-Φ IM are written [17]

$$v_{qs} = i_{qs}r_s + \omega\lambda_{ds} + \frac{d\lambda_{qs}}{dt} \quad (15)$$

$$v'_{qr} = i'_{qr}r'_{qr} + (\omega - \omega_r)\lambda'_{dr} + \frac{d\lambda'_{qr}}{dt} \quad (16)$$

$$v_{ds} = i_{ds}r_s + \omega\lambda_{qs} + \frac{d\lambda_{ds}}{dt} \quad (17)$$

$$v'_{dr} = i'_{dr} + (\omega - \omega_r)\lambda'_{qr} + \frac{d\lambda'_{dr}}{dt} \quad (18)$$

where " ' " represent rotor quantities referred to stator side.

Also, let quantity E_{xy} represent various d-q parameters where 'E' can be flux-linkage λ, voltage *v* & current *i*; 'x' can be 'd' or 'q' ; 'y' can be 'r' & 's'. Here'd' represent d-axis quantities & 'q' represent q-axis quantities. Further 'r'&'s' represents quantities for rotor & stator respectively.

Now the equations for flux linkages are given by [17];

$$\begin{pmatrix}\lambda_{qs}\\ \lambda_{ds}\\ \lambda'_{qr}\\ \lambda'_{dr}\end{pmatrix} = \begin{pmatrix}L_m + L_{ls} & 0 & L_m & 0\\ 0 & L_m + L_{ls} & 0 & L_m\\ L_m & 0 & L_m + L'_{lr} & 0\\ 0 & L_m & 0 & L_m + L'_{lr}\end{pmatrix}\begin{pmatrix}i_{qs}\\ i_{ds}\\ i'_{qr}\\ i'_{dr}\end{pmatrix} \quad (19)$$

where, L_m is the magnetizing inductance (H), L_{ls} is the leakage inductance of stator winding (H) and L'_{lr} is the the leakage inductance of rotor winding referred to stator (H).

The electromagnetic torque 'm_d' developed in induction motor is expressed as [17],

$$m_d = \frac{3}{2}\frac{p}{2}\frac{L_m}{L_s}(\lambda_{qs}i'_{qr} - \lambda_{ds}i'_{qr}) \quad (20)$$

$$J\frac{d\omega_r}{dt} + B\omega_r + m_L = m_d \quad (21)$$

where *p* is the number of poles of the machine , *J* is the moment of inertia (kg-m^2), ω_r is the rotor angular electrical speed (rps) and m_L is the centrifugal pump load, which can be given by,

$$m_L = K\omega_r^2 \quad (22)$$

where K is centrifugal pump constant.

IM is simulated in synchronous reference frame. Here v'_{qr} , v'_{dr} are equal to zero as we are using squirrel cage induction motor, in which rotor terminals are shorted.

III. CONTORL STRATEGY AND MPPT ALGORITHM

In the proposed system PV power is conditioned by cascaded MLI. MLI not only conditions the PV power into required high quality three phase output required for IM but it also operates the PV source near MPPT. Below gives the detail description for the MPPT algorithm and the respective control strategy used in the proposed system.

A. MPPT algorithm

The utilization of solar PV panel is hindered by the fact that the relation between power versus voltage curve for solar array is non-linear. PV source has maximum power point at a particular operating voltage which varies with the insolation and temperature. Maximum Power Point Tracker maintains the PV source near optimum voltage to deliver the maximum power to the load at different values of insolation and temperature. Proposed work senses PV voltage 'v_{pv}' and

current 'i_{pv}' as input parameters to track Maximum Power Point (MPP). Depending on the average value of the two parameters, MPPT controller modifies the value of modulation index 'm_a' as given in the Fig. 4. The value of m_a is further processed by SPWM controller for defining the output voltage and frequency for the inverter. MPPT algorithm is based on simple P & O method where MPPT controller modifies the m_a [18-19] with respect to sensed PV voltage and current. Flowchart for the MPPT algorithm used in the proposed model is shown in Fig. 4.

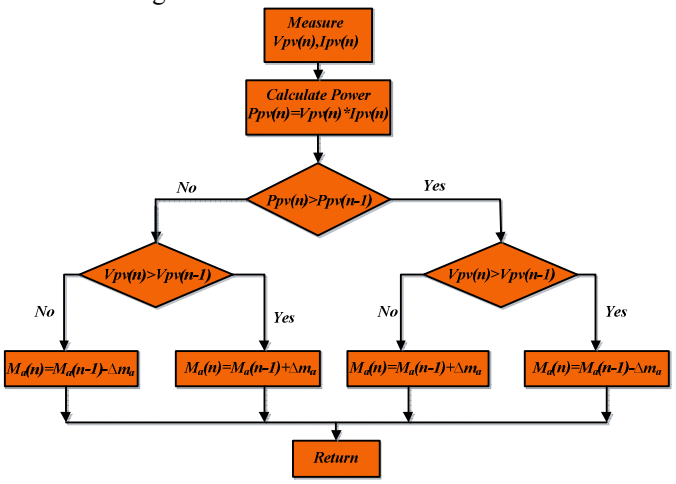

Fig. 4. The flowchart of the proposed MPPT method

B. *Sinusoidal Pulse Width Modulation (SPWM) Technique*

The m_a value calculated by the MPPT algorithm is used by SPWM technique. The value of m_a apart from defining the magnitude it is also frequency calculation of applied phase voltage with respect to *V/f* control. The reference modulating signal is compared with carrier wave and switching signals are generated for inverter-1 and inverter-2 as shown in Fig. 5. In SPWM, three sinusoidal modulating waves corresponding to the required output voltage are compared with two carrier waves corresponding to the switching frequency of the device as shown in Fig. 5. The switching logic used by PWM technique [20] is for 'a' phase of inverter is also given in Fig. 5. For inverter leg connected to phase 'a', it can be observed that when modulating sine wave is greater than or equal to the upper carrier wave S_{11} & S_{13} are ON; when modulating sine wave is greater the lower carrier wave and less than or equal to the upper carrier wave S_{12} & S_{13} are ON and the switch S_{14} is ON when the modulating sine wave is less than or equal to the lower carrier wave.

IV. SIMULATION RESULTS AND ANALYSIS

In simulation, the proposed system consist of 60 modules where each module has the specification of V_{oc}=21V, I_{sc}=3.74A, V_m=17.1V, I_m=3.5A, P_m=59.9W, at Standard Test Conditions (STC). Of these 60 modules 15 are connected in series to form PV panel. Two such panels are again connected in parallel which forms PV array. Two such PV arrays are used by the cascaded MLI which is further connected to the three-phase motor pump load.

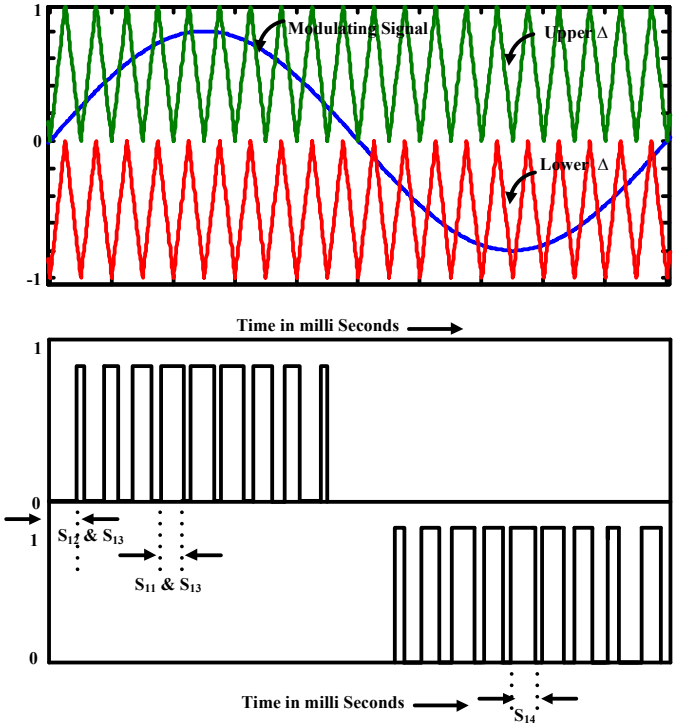

Fig. 5. PWM Switching Strategy for the proposed system, for m_a=0.8

Three phase motor pump used has rating of 4-pole, 400V, 4kW, 1430 rpm, 3-Ø induction motor. The proposed system is simulated for increasing and decreasing trend of four different insolation 0.3Sun, 0.6Sun, 1Sun, 0.8Sun and temperatures of 26^0C, 32^0C, 45^0C, 42^0C respectively. Fig. 6 shows the simulation results of the proposed system at different environmental conditions for PV source side parameters. DC-bus capacitors are initially assumed to be uncharged; hence the initial PV current drawn is equal to the short circuit current. Some of the important observations that can be observed in the simulation results of Fig. 6 and Fig. 8 are as follows:

When the environmental condition varies, the PV power varies instantaneously, but the load side parameter doesn't vary in synchronism with PV power. During this transient period, DC-bus capacitors play a crucial role by absorbing the excess PV power when insolation is increased and supplies deficit power to the load, when insolation is decreased. When the insolation increases, PV power increases as PV current varies in proportion with insolation. During this period DC-bus capacitors charges to V_{oc} by absorbing excess PV power and there by PV enters into the voltage source region, thus resulting in sudden decrease in PV power, which appears a spike in PV power plot of Fig. 6. And there from it tracks mpp.When the insolation decreases, PV power decreases as PV current varies in proportion with insolation, thus DC-bus capacitors discharges in order to supply deficit power to the load resulting in sudden dip in DC-bus voltage of PV voltage, hence PV enters into current source region and there from it tracks MPP. During this transient period PV power is less than the output power hence a sudden spike in efficiency beyond 100% can be observed in efficiency plot of Fig. 8. When the

MPP is tracked, m_a perturbs around its optimum value. The perturbation in m_a causes oscillations in v_{pv}, i_{pv} and p_{pv}. Further, it can be observed that the oscillating frequency of the p_{pv} is twice the oscillating frequency of v_{pv} and i_{pv}. The magnitude of oscillations in above parameter depends on Δm_a allowed. The choice of selecting Δm_a is based on two important factors, if its value is kept low, the magnitude of oscillations in v_{pv}, i_{pv} and p_{pv} will be minute but the tracking speed of MPP decreases. On the other hand if Δm_a is selected high, we can obtain good tracking speed but with higher magnitude oscillations resulting in deteriorated performance of motor. Fig. 8 shows the motor side parameters for different environmental conditions.

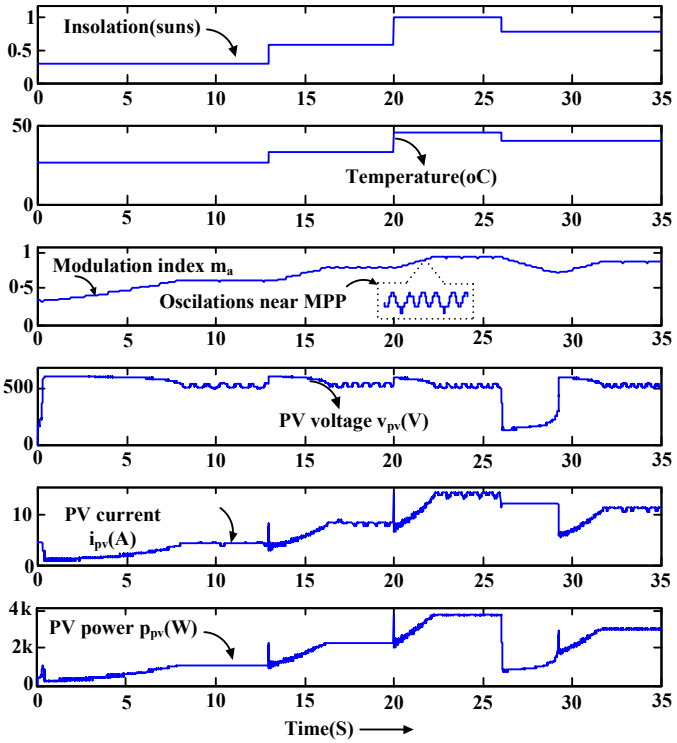

Fig. 6. Simulation results at PV source side.

One of the factor by which induction motor performance can be judged is by amount of ripples in speed, torque and power. These are determined by the motor phase voltage and current. SPWM allows the inverter to operate in 3-level mode of inversion at all values of m_a, as shown in Fig. 7, hence produces lower harmonic distortion in the motor phase currents as shown in Fig. 9, and there by reduces ripples in torque. The motor phase voltage and current envelops are similar to PV voltage and current variations, as it can be observed from simulation results, hence lower magnitude of oscillations in PV voltage and current improves the performance of induction motor. Induction motor torque and speed depends on V and f fed to it, which in turn depends on m_a. Hence the variation in power output, torque and speed of motor follows the same trend in which m_a varies. Further it, can be observed that m_a settles at higher values deriving higher PV power at higher insolation and it settles at low values deriving low PV power at lower insolation.

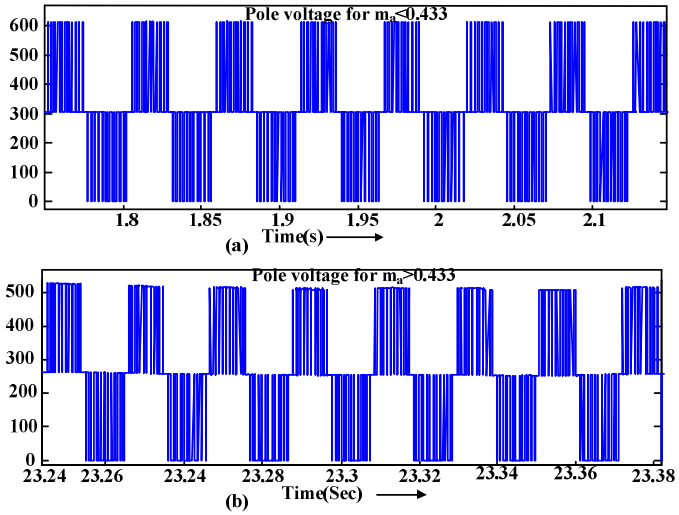

Fig. 7. Pole voltage showing 3- level operation at (a) m_a=0.37 and (b) m_a=0.945

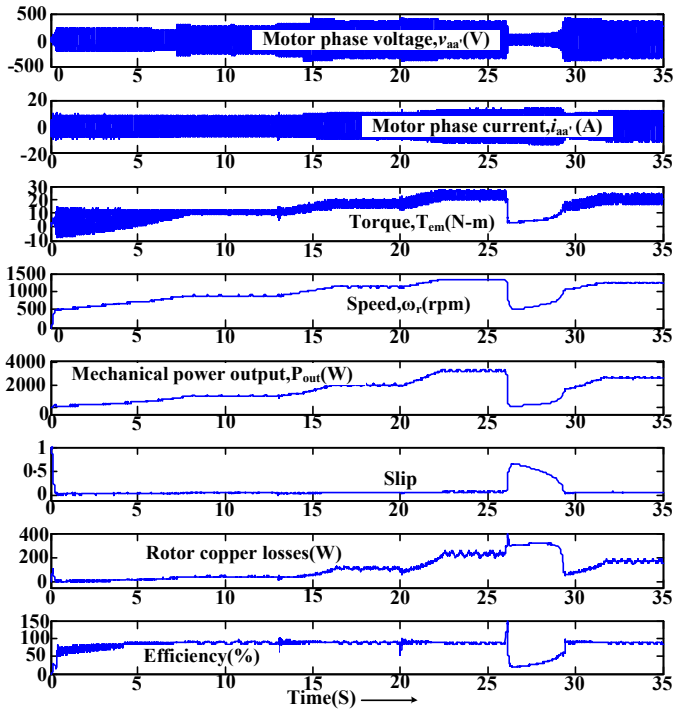

Fig. 8. Simulation results at motor pump side.

One of the important advantages of the proposed system is, the magnitude of rotor copper losses in induction motor vary in accordance with the magnitude of PV power derived which can be observed in Table I. At lower insolation, PV power derived is low and there by the corresponding rotor copper losses also reduce, hence utilizing PV power efficiently even at lower insolation also. Finally the proposed system transmits PV power to the load at higher efficiency at all values of m_a as it can be observed in Table I. Table I gives the clear insight of the proposed system and the readings mentioned/ noted at steady state. Fig. 9. Shows the harmonic analysis of phase currents fed to the IM by the proposed system and it can be observed that the ripples in the phase currents decreases at higher insolation.

TABLE I. Tabular analysis of the proposed system obtained from Fig. 6 and Fig. 8.

G(Suns)	T (°C)	ma	F (Hz)	N_s (rpm)	N_r (rpm)	Torque (N-m)	Wcu (W)	Ppv (W)	Pout (W)	η(%)	% Silp
0.3	26	0.62	31	930	890	10.8	44	1123	1000	89	4.3
0.6	32	0.79	39.75	1192	1130	17	110	2295	2000	87	5.1
0.8	40	0.87	43.75	1312	1240	20.5	170	3035	2650	87	6
1	45	0.94	47.25	1417	1328	23.5	230	3765	3250	86	6.5

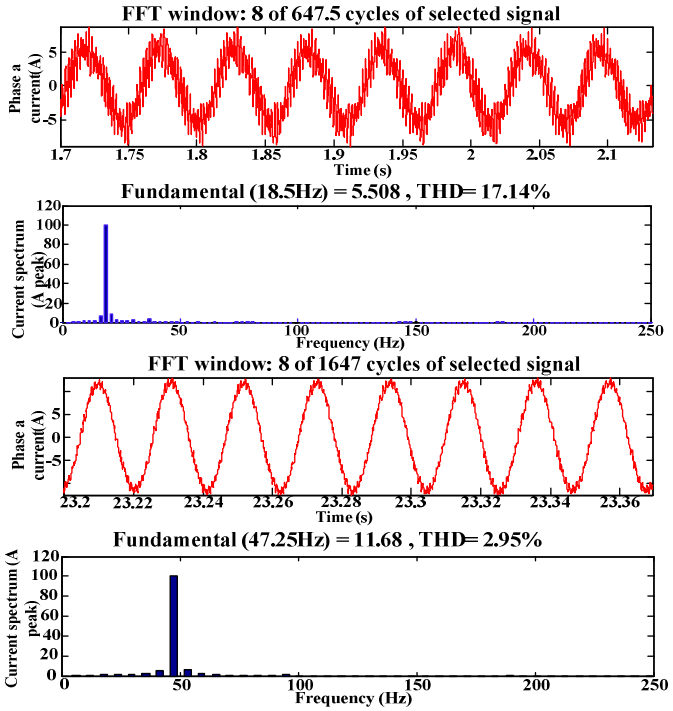

Fig. 9. Motor a-phase current and its harmonic spectrum.

V. CONCLUSION

In this study an optimal and efficient single- stage integrated PV system feeding centrifugal pump load is presented. A simple MPPT algorithm and *V/f* control strategy has been used, which makes the system to operate at higher efficiencies. SPWM technique has been preferred over SVPWM, as it always makes the inverter to operate in 3-level irrespective of m_a value hence produces the required input quantities to the induction motor with less ripple content in it, whereas SVPWM makes inverter to operate in 2-level mode for m_a <0.433. A detailed yet simple mathematical modeling of inverter and its integration with PV module has been implemented for simulation in MATLAB/Simulink. The simulation results demonstrated that it is possible to operate the system at MPPT for varying insolation and temperatures with simple control strategy.

REFERENCES

[1] Sefa I, Altin N, "Grid interactive photovoltaic inverters—a review," J Fac Eng Archit Gazi Univ 2009; 24(3):409–24.

[2] Ibrahim Sefa, Mehmet Demirtas, Ilhami Çolak, "Application of one-axis sun tracking system," Energy Convers Manage 2009; 50:2709–18.

[3] Jih-Sheng Lai, and Fang Zheng Peng, "Multilevel Converters-A New Breed of Power Converters," *IEEE Trans. on Ind. Appl.*, vol. 32, no. 3, May/June 1996.

[4] Rodriguez J,Lai JS, Peng FZ, "Multilevel inverters: a survey of topologies,controls, and applications,"*IEEE Trans Ind Electron* 2002., vol. 49, no. 4, Aug 2002; 49(4):724–38.

[5] Dixon J, Morán L, "High-level multistep inverter optimization using a minimum number of power transistors," *IEEE Trans Power Electron* vol. 21, no. 2, Mar 2006; 21(2):330–7.

[6] Babaei E, Moeinian MS, "Asymmetric cascaded multilevel inverter with charge balance control of a low resolution symmetric subsystem," Energy Convers Manage 2010; 51:2272–8.

[7] Colak I, Kabalci E, Bayindir R, "Review of multilevel voltage source inverter topologies and control schemes," Energy Convers Manage 2011; 52:1114–28.

[8] Nabae A., Takahashi I, Akagi H, "A new neutral-point clamped PWM inverter," *IEEE Trans. Ind. Appl.* **17**(5), 518–523 (1981).

[9] Carpita, M.; Tenconi, S.; "A novel multilevel structure for voltage source inverter," Proc. EPE1991.

[10] Choi,N.S.; Cho, J.G.;Cho, G.H.; "Ageneral circuit topology of multilevel inverter," Proc. Power Electron. Spec. Conf. 96–103 (1991).

[11] Meynard, T.A.; Foch, H.: Multi-level conversion: high voltage choppers and voltage-source inverters. Proc. IEEE Power Electron.Spec. Conf. 1992; 397–403.

[12] Hammond, P.W.: "A new approach to enhance power quality for medium voltage ac drives," *IEEE Trans. Ind. Appl.* 1997; **33**(1), 202–208.

[13] Peng, F.Z.; Lai, J.; Mckeever, J.; Vancoevering, J.: "A multilevel voltage-source inverter with separate dc sources for static var generation," Proc. IEEE IAS Annu. Meet. **3**, 1995; 2541–2548.

[14] V.T.Somasekhar and K.Gopakuma "Three-level inverter configuration cascading two-level inverters", *IEE Proc. of Electr. Power Appl.,* Vol.150, No.3,May 2003, pp.245-254.

[15] G.R. Walker, "Evaluating MPPT Topologies Using a Matlab PV model", Journal of Electrical & Electronics Engineering, 2001;Vol. 21, No. 1, pp. 49-56,.

[16] Byoung-kuk Lee, Ehsami. M, "A simplified functional simulation model for three-phase voltage source inverter using switching function concept," *IEEE Trans. Ind. Elect.*, vol. 48, no. 2, pp. 309-321, Apr. 2001.

[17] P. C. Krause, O. Wasynczuk, S. D. Sudhoff "Analysis of Electric Machinery and Drive Systems", IEEE Press, A John Wiley & Sons, Inc. Publication Second Edition, 2002.

[18] X. Liu and L. A. C. Lopes, "An improved perturbation and observation maximum power point tracling algorithm for PV anrays," presented at Power Electronics Specialists Conference, 2004. PESC 04. 2004 IEEE.35th Annual, 2004.

[19] S.Jain and V.Agarwal ,Comparison of the performance of maximum power point tracking schemes applied to single stage grid-connected photovoltaic systems" *IET Electr. Power Appl.,* 2007, 1, (5), pp. 753–762.

[20] Leon M.Tolbert and Thomas G. Habetler," Novel Multilevel Inverter Carrier-Based PWM Method," *IEEE Trans. Ind. Appl.* vol. 35, no. 5, pp. 1098-1107, Sept/Oct. 1999.